Ocean Sci., 9, 261–279, 2013
www.ocean-sci.net/9/261/2013/
doi:10.5194/os-9-261-2013

Ocean Science Open Access

Towards an integrated forecasting system for fisheries on habitat-bound stocks

A. Christensen[1], **M. Butenschön**[2], **Z. Gürkan**[1], **and I. J. Allen**[2]

[1]DTU Aqua, Technical University of Denmark, 2920 Charlottenlund, Denmark
[2]Plymouth Marine Laboratory, Prospect Place, The Hoe, Plymouth PL1 3DH, UK

Correspondence to: A. Christensen (asc@aqua.dtu.dk)

Received: 1 March 2012 – Published in Ocean Sci. Discuss.: 30 March 2012
Revised: 29 December 2012 – Accepted: 15 January 2013 – Published: 7 March 2013

Abstract. First results of a coupled modelling and forecasting system for fisheries on habitat-bound stocks are being presented. The system consists currently of three mathematically, fundamentally different model subsystems coupled offline: POLCOMS providing the physical environment implemented in the domain of the north-west European shelf, the SPAM model which describes sandeel stocks in the North Sea, and the third component, the SLAM model, which connects POLCOMS and SPAM by computing the physical–biological interaction. Our major experience by the coupling model subsystems is that well-defined and generic model interfaces are very important for a successful and extendable coupled model framework. The integrated approach, simulating ecosystem dynamics from physics to fish, allows for analysis of the pathways in the ecosystem to investigate the propagation of changes in the ocean climate and to quantify the impacts on the higher trophic level, in this case the sandeel population, demonstrated here on the basis of hindcast data. The coupled forecasting system is tested for some typical scientific questions appearing in spatial fish stock management and marine spatial planning, including determination of local and basin-scale maximum sustainable yield, stock connectivity and source/sink structure. Our presented simulations indicate that sandeel stocks are currently exploited close to the maximum sustainable yield, even though periodic overfishing seems to have occurred, but large uncertainty is associated with determining stock maximum sustainable yield due to stock inherent dynamics and climatic variability. Our statistical ensemble simulations indicates that the predictive horizon set by climate interannual variability is 2–6 yr, after which only an asymptotic probability distribution of stock properties, like biomass, are predictable.

1 Introduction

In recent years evidence of degradation of marine ecosystems by overfishing, by-catch, climate change, eutrophication and chemical pollution from land runoff, coastal development, habitat destruction and other human activities has become undisputable (Levin and Lubchenco, 2008). Why are we still uncertain about how best to manage the crisis of ecosystems, especially fish communities, triggered directly or indirectly by human impacts? Forecasting fish stocks, akin to the ubiquitous weather forecasts, has proved to be an elusive target for fishery science (Huse and Ottersen, 2003; Megrey et al., 2005). This is fundamentally related to the character of the ecosystem dynamics where the processes are poorly constrained, quantified and partially still poorly understood, and involve ranges of temporal/spatial scales that span several orders of magnitude, generally non-linearly linked. A key problem here remains the insufficient field sampling of ecosystem state variables to parametrize processes, define its initial state and boundary conditions as well as insufficient spatial resolution of ecosystem models (Fulton et al., 2003). Consequently, fundamental difficulties in analyzing ecosystem behaviour arise and hypotheses are numerous and difficult to discriminate (Carpenter, 2002), further complicated by mathematical issues typical of non-linear systems like instabilities, chaos and regime shifts. These pessimistic prospects have spurred some interest in alternative routes to ecosystem forecasting, like artificial neural networks (Chen and Ware, 1999; Huse and Ottersen, 2003; Suryanarayana et al., 2008). However, ecosystems are facing regime shifts and major trophic reorganization these years (Beaugrand et al., 2002; Alheit, 2009; Kenny et al., 2009; Moellmann et al.,

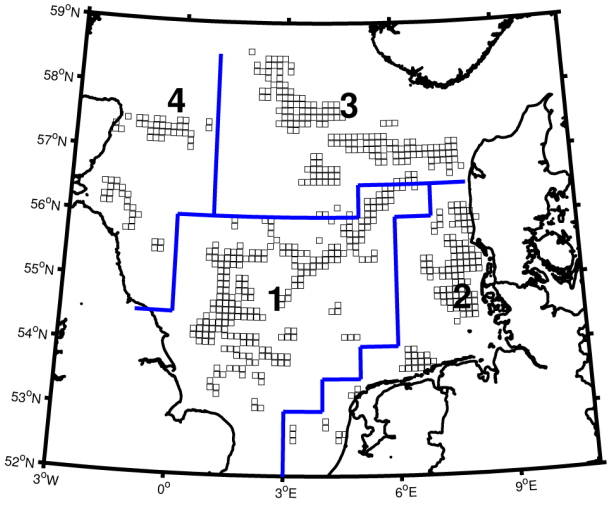

Fig. 1. Small boxes show suitable sandeel habitats resolved on a 10 km scale corresponding to the POLCOMS grid. The habitat network is represented by 585 such cells, which is the model domain of the SPAM model. The lines indicate WGNSSK regional stock assessment areas 1–4.

2009), which renders— unguided machine learning from recent history dubious; there is no safe way around improving a process-oriented representation of the marine ecosystems.

Despite not being on the mark yet, many advances in process-oriented ecosystem modelling have been presented recently (Fulton et al., 2011; Hinrichsen et al., 2011). Many of these advances are supporting operational systems of physical regional circulation models and associated biogeochemical models describing the lower trophic ecosystem levels (Gallego et al., 2007; Brasseur et al., 2009) which provide access to high quality input data for fish stock models. The process of integrating operational oceanography products with fish stock models has been accelerated by projects like MyOcean (MyOcean, 2009–2012).

Even though many impressive models describing complex fish stocks, like tuna (Lehodey et al., 2008; Senina et al., 2010; Lehodey et al., 2010), have been put forward, many fundamental issues remains unresolved and too many important processes are aggregated in model constructions. To achieve a better understanding of fish stock dynamics, it is attractive to focus on fish species with comparatively simple life cycles and then transfer experiences to fish species displaying more complex traits as well as interacting fish stocks. Here sandeel and other sedentary species with well-characterized habitat requirements appear ideal, because stock migration is a very challenging issue to model (Kishi et al., 2011). Ecologically, sandeel is an important mid-trophic wasp-waist species, capable of exerting both bottom-up and top-down control, in that it constitutes a significant part of the fish biomass ($\sim$ 25 %) in the North Sea ecosystem. Therefore, predicting and understanding the dynamics of this stock has attracted some interest (van Deurs et al., 2009; Arnott and Ruxton, 2002; Lewy et al., 2004), however most of these works are statistical approaches. Lewy et al. (2004) found that the predictability of all the North Sea sandeel stocks together was better than that of individual substocks; our work will challenge this finding. The short life cycle of the species makes it especially susceptible to spatial and temporal variability in ambient physical conditions, because the biomass and recruitment are controlled by one or two offspring cohorts (Arnott and Ruxton, 2002). For instance, in 2010 the proportion of fish just one year old in the catch was more than 90 %, and such a high proportion has been observed in other years as well (WGNSSK, 2011). Sandeel stocks display strong interannual fluctuations, often biomass changes by more than a factor of two between years. In addition to this, North Sea sandeel biomasses have historically experienced an apparent regime shift (Grandgeorge et al., 2008; van Deurs et al., 2009), going from a high average abundance level ($\sim$ 2 Mt) to a lower average abundance level ($\sim$ 1 Mt) around 1998–1999 (WGNSSK, 2011). The exact reason for this has not unambiguously been resolved, even though fishing pressure increased prior to the regime shift. However, other fish stocks predating sandeels (Beaugrand et al., 2003), as well as the North Sea zooplankton composition (Beaugrand et al., 2002), experienced preceding regime shifts, pointing in the direction of trophic cascades. Sandeels are fished for fish meal and fish oil production. They bury in the sandy sea bed when not feeding, and therefore these stocks are localized to areas with sandy bottom substrate. These habitats have been mapped in detail from fishery log books (Jensen and Rolev, 2004), see Fig. 1.

The temporal and spatial variability of the North Sea sandeel stocks makes this case study a rigorous test of the current capability of forecasting fish stocks. Such a variable resource poses a great challenge to an economical sector requiring a relatively constant supply to operate with low cost levels. Predicting stock dynamics on a short timescale of 1–2 yr would be of great value to fishermen and industry, allowing them to anticipate inherent stock fluctuations and reallocate catch effort in time to other opportunities. Current fish stock assessment is data driven with limited spatial resolution (i.e. regional- or basin-scale).

Marine spatial planning often requires knowledge about ecosystem properties and responses at subregional scales (< 50 km), and there is a pressing need to know how fish stocks respond to management actions and human activity on these smaller scales.

In this paper we present a spatial fish stock forecasting system addressing the needs above that can run in either hindcast/forecast mode or in reanalysis mode with a simple data assimilation scheme for the purposes of

- providing short-term forecasts including the effects of seasonal and interannual variability;
- providing a flexible tool for assessing effects of alternative scenarios of stock management, involving both local-scale and basin-scale management actions; and
- downscaling regional-scale stock assessments to provide access to stock variability on spatial scales < 50 km which is not accessible through regional-scale stock assessments.

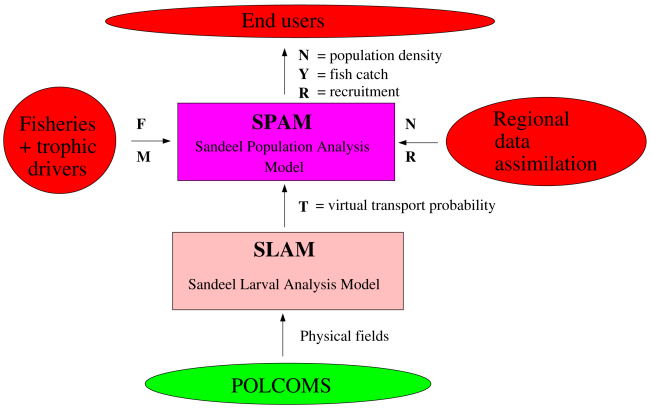

Fig. 2. Diagram of coupled model elements.

2 Forecasting model system

The forecasting system targeting habitat-bound fish stocks presented here contains three elements as depicted in Fig. 2: at the bottom, ocean physics is provided by the POLCOMS model; at the top, fish stocks and fisheries are described by the SPAM model; the top and the bottom are glued together by the SLAM model, describing early life stages of fish stocks. All three model components are described below and are coupled offline, as described in Sect. 2.4. In this way all of the pathway from climate to fish landings is described by the system. We illustrate the forecasting model system on North Sea sandeel stocks. Challenges involved in generalization of the forecasting system to other species are addressed in Sect. 4. The biological models (SLAM and SPAM) represents a light-weight but balanced choice between explicitly represented processes and aggregated processes, since defaulting to the finest resolution and greatest complexity in all the dimensions (e.g. spatial, temporal, taxonomic, process detail) is not beneficial (Fulton, 2010) because uncertainties in additional processes may lead to degradation for overall model performance.

2.1 Physics

The hydrodynamic environment for the sandeel population is given by an implementation of the POLCOMS modelling system (Allen et al., 2001) implemented on the NW European shelf (Butenschön et al., 2012). This model is a further development of the MyOcean v0 model (Siddorn et al., 2007) for the NW European seas that provides an enlarged domain corresponding to the v1 model (Edwards et al., 2012), allowing for a more realistic representation of the impacts of the shelf exchange processes on the shelf waters (Holt et al., 2012), and uses a consolidated version of POLCOMS. POLCOMS is a primitive equation model for the coastal ocean using sigma coordinates and a Arakawa B-grid with a piecewise parallel scheme for advection processes. Turbulence closure is achieved through the Mellor–Yamada model with an algebraic mixing length. Details on this part of the modelling system and extensive validation of its forecasting quality are given in the above mentioned references. From a model hindcast of the years 1960–2004, only the years 1970–2004 were used for this work to exclude spin-up effects. Figure 3 shows spatial and interannual temperature distribution to illustrate a major environmental impact factor on the sandeel habitats (see Fig. 1). The POLCOMS modelling system is coded in Fortran 90 to ensure high computational performance.

2.2 SLAM (Sandeel Larval Analysis Model)

SLAM (Sandeel Larval Analysis Model) is an individual-based model describing transport and survival probability of early life stages (fish eggs and larvae) of sandeel (Christensen et al., 2008).

Sandeels have pelagic larvae, and their physical transport is described by passive advection–diffusion in this work. Larval trajectories were generated by Euler forward integration using a time step of 1800 s, which has been found to generate sufficiently accurate trajectories previously. Larval hatching date is set to 20 February, based on biological observations (Wright and Bailey, 1996; Jensen, 2001). Larval growth is described by a temperature-controlled growth model (model 3 in Table 2 in Christensen et al., 2008), where temperatures are obtained from the coupled POLCOMS model. In the SLAM model larvae settle when they reach the length of metamorphosis $L = L_{\mathrm{m}}$ (Wright and Bailey, 1996; Jensen, 2001), if they are at in suitable habitat (Fig. 1) according to the temperature-controlled growth model – otherwise they are lost (biologically they have a high mortality). This and alternative growth models were compared extensively in a previous work (Christensen et al., 2008), and results were found to be relatively insensitive to model details. All other details of the computational set-up were identical to previous work (Christensen et al., 2008). By hatching larvae from all suitable 585 habitat cells in Fig. 1, a 585×585 transport matrix $\mathbf{T}^{\mathrm{y}}$ is generated by the SLAM

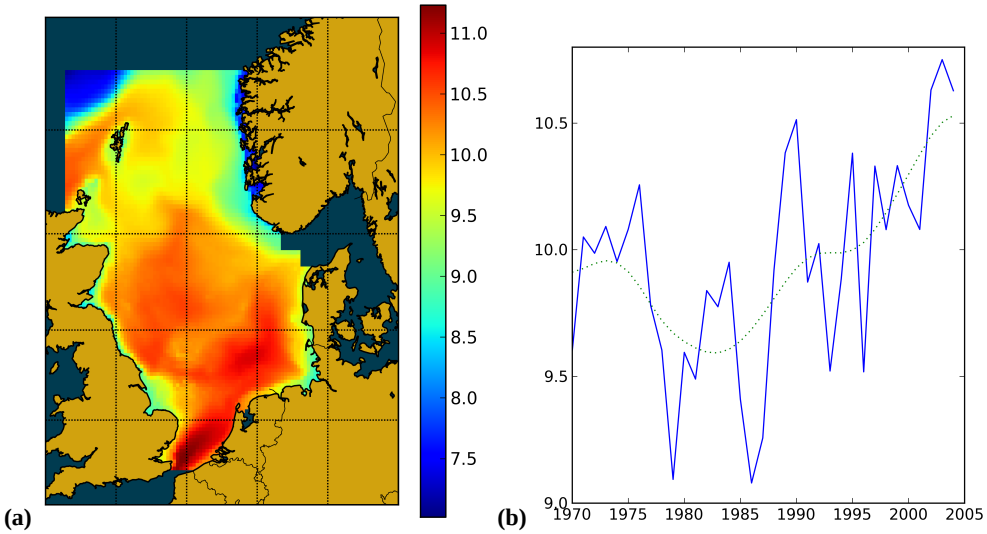

Fig. 3. (a) Temporally averaged temperature (°C), 1970–2004, from POLCOMS, averaged over depth. **(b)** Spatially averaged temperature (°C), 1970–2004, from POLCOMS.

model for each year "y" describing habitat connectivity. For each year, $n = 1000$ larvae per habitat cell were used to sample the transport matrix, so that a yearly transport simulation encompassed 585 000 released particles. Basic probability theory gives that the relative uncertainty $\mathrm{RMS}(T_{ij})/T_{ij}$ on a transport probability T_{ij} obtained by sampling is $1/\sqrt{nT_{ij}}$, so that very rare transport pathways are less accurately resolved; on the other hand they do not contribute much to biomass dynamics (in most cases). A database $\mathbf{T}^{\mathrm{y}}$ was generated for y = 1970–2004 from POLCOMS output to span climatic variability (thus also including temperature-controlled larval growth). These transport matrices were the input the stock model SPAM (see below) used to calculate spatial recruitment of new generations. The SLAM model addresses density independent growth and mortality processes. The model SPAM (see below) corrects for density dependence on larval growth and mortality (van Deurs et al., 2009). The SLAM model is coded in modular Fortran 90 to ensure high computational performance.

2.3 SPAM (Sandeel Population Analysis Model)

SPAM (Sandeel Population Analysis Model) is a spatial stock model for settled sandeel that follows cohorts (generations) through their life cycle. The SPAM model was previously parametrized for a regional-scale set-up (Christensen et al., 2009), whereas this work presents a high resolution set-up on a 10×10 km grid, coincident with the physical grid used for the POLCOMS hindcast, so that spatial resolution of all three model components is aligned. The 10 km grid scale allows for emergence of fine-scale spatial biological patterns; limited biological data only allows biological parameters to be varied on regional or North Sea scale, otherwise the model becomes over-parametrized.

The state variables in the SPAM framework are the abundance $N^{\mathrm{y}}_{i,\mathrm{a}}$ and average fish length $L^{\mathrm{y}}_{i,\mathrm{a}}$ in each habitat cell i in Fig. 1 for each generation with age "a" and for each year "y". The present set-up comprises 596 habitat cells each having 12 age classes. The state variables describe conditions on 1 January each year, so they represent time snapshots and not averages over the year. State variables are updated from 1 January to 1 January the subsequent year by integrating processes over the elapsed year. The SPAM model and its parametrization were thoroughly discussed in (Christensen et al., 2009), and we adhere to the notation established there and provide a summary along with developments in Appendix A. The SPAM model can run as a standalone life cycle model in hindcast mode or in reanalysis mode with various degrees of data assimilation. The time integration step in the SPAM model is:

$$N^{\mathrm{y}+1}_{i,\mathrm{a}+1} = \delta_{\mathrm{a},0} \sum_j R^{\mathrm{y}}_{ij} + e^{-Z^{\mathrm{y}}_{i,\mathrm{a}}} N^{\mathrm{y}}_{i,\mathrm{a}} \tag{1}$$

$$L^{\mathrm{y}+1}_{i,\mathrm{a}+1} = L^{\mathrm{y}}_{i,\mathrm{a}} + g\left(L^{\mathrm{y}}_{i,\mathrm{a}}, N^{\mathrm{y}}_{i,\mathrm{a}}\right) \tag{2}$$

$$R^{\mathrm{y}}_{ij} = T^{\mathrm{y}}_{ij} S^{\mathrm{y}}_{ij} \sum_{\mathrm{a}} Q^{\mathrm{y}}_{j,\mathrm{a}} N^{\mathrm{y}}_{j,\mathrm{a}}, \tag{3}$$

where $Z = F + M + Z_0$ is the total mortality composed of fishing pressure F, predation M and background (other) mortality Z_0. δ is the Kronecker delta. R is the recruitment (of a new generation), which is assembled in SPAM from the transport matrix $\mathbf{T}$ passed from SLAM, and fecundity Q and conditional survival chance $\mathbf{S}$, both of which depends on N and L. The primary forcings of the model are ($F^{\mathrm{y}}_{i,\mathrm{a}}$, $M^{\mathrm{y}}_{i,\mathrm{a}}$,

T^{y}_{ij}). The indirect forcings are the habitat carrying capacity C^{y}_i (see Appendix A for model parametrization details, where also the length-specific growth parametrization g_i is described). Especially in Appendix A, we describe attempts to parametrize growth in relation to zooplankton abundance. In addition to dependence on length and stock size, it was tested whether growth g depended on zooplankton (i.e. food) density and temperature; however, observations did not support a significant relation (see Appendix A for further details). A useful diagnostic quantity that we will discuss later is the recruit-per-recruit number r^{y}_i,

$$r^{\mathrm{y}}_i = \sum_{\xi>\mathrm{y},\,\mathrm{a}>1} \sigma^{\xi}_{i,\xi-\mathrm{y}} Q^{\xi}_{i,\xi-\mathrm{y}} \sum_j T^{\xi}_{ji} S^{\xi}_{ji}, \tag{4}$$

where

$$\sigma^{\xi}_{i,\xi-\mathrm{y}} = e^{-\sum_{\xi>\mathrm{y}} Z^{\xi}_{i,\xi-\mathrm{y}}} \tag{5}$$

which is the future number of (somewhere) settled offspring that a new juvenile can expect to produce in its lifetime, given that it settles in habitat cell i at year "y", and $\sigma^{\xi}_{i,\mathrm{a}}$ is the probability of surviving to age "a" at year ξ, given settlement in habitat i. r^{y}_i is a function of fishing mortality $F^{\xi>\mathrm{y}}_{i,\mathrm{a}}$ (in addition to state matrices $\mathbf{N}^{\xi>\mathrm{y}}$ and $\mathbf{L}^{\xi>\mathrm{y}}$). In relation to stock management, it is interesting to see at what fishing pressure $r = 1$, i.e. when a newly settled juvenile closes its life cycle with one new recruit on average.

$$\psi^{\mathrm{y}}_i = F^{\xi>\mathrm{y}}_{i,\mathrm{a}} : r^{\mathrm{y}}_i \left(F^{\xi>\mathrm{y}}_{i,\mathrm{a}} \right) = 1 \tag{6}$$

This defines a local maximum sustainable fishing pressure. For sinks, Eq. (6) will not have a solution (thus identifying sinks, using this definition).

The SPAM model is written as a Python class library. Simulating stock dynamics at the present spatial resolution takes less than half a second per year on a standard laptop, thus enabling extensive ensemble simulations at high spatial resolution.

2.4 Coupling models

It is important to realize that the three elements in the present forecasting system are fundamentally very different and address different temporal and spatial timescales: POLCOMS is an Eulerian model based on the continuum hypothesis solving the balances for mass, momentum and energy in the form of partial differential equations, while SLAM is a Lagrangian framework and SPAM implements discrete difference equations of stock dynamics. Therefore, at a technical and mathematical level the coupling of the three elements is by no means trivial and requires well-defined interfaces. In this work, the models are coupled offline, meaning that models are run independently, as opposed to being coupled online where models are run contemporaneously (and exchange data bidirectionally). In this work, data exchange between POLCOMS and the SLAM models occurs in daily 3-D time frames of average ocean fields; the SLAM-SPAM interface exchanges yearly transport matrices $\mathbf{T}^{\mathrm{y}}$ and $\mathbf{S}^{\mathrm{y}}$. Further aspects of online versus offline coupling are discussed in the Sect. 4.

2.5 Stock data and data assimilation

Recently, the ICES Working Group on the Assessment of Demersal Stocks in the North Sea and Skagerrak (WGNSSK, 2011) moved from basin-scale to regional-scale assessment of sandeel stocks in ICES area IV, based on statistical analysis of catch landings, catch sampling and biological surveys. ICES WGNSSK adopted a regional division of the sandeel habitat network, see Fig. 1, partially based on hydrographic connectivity. In areas $A = 1$–3, SSB_A (spawning biomass of age $\geq$2, see Eq. A3), TSB_A (total adult biomass of age $\geq$1, see Eq. A4), recruitment (R_A), catches Y_A and average weight at catch were reported for 1983–2010; in area 4 only catches for 1983–2010 were reported. The time series of SSB, TSB, and R for 1983–2010 have a quite decent overlap with the POLCOMS hindcast of physics (1970–2004) to enable reanalysis runs. These WGNSSK fish stock assessments are considered as pseudo observations that can be assimilated independently in SPAM in reanalysis mode.

Data assimilation techniques are widely used in geosciences modelling and refer to a wide range of techniques for model reanalysis, starting from direct insertion and nudging, advancing to Kalman filters and variational methods (Robinson and Lermusoaux, 2000). Crude direct insertions replace model state variables with observations assuming no observational error, while nudging relaxes the model's state toward observations using a prescribed relaxation pace. A popular basis is the Kalman filter (see, e.g. Larsen et al., 2007). The basic problem in our context is that basic premises of the Kalman filter are not satisfied (system linearity and unbiased multivariate Gaussian error structure), and therefore adaptation and extensive testing will be necessary to apply this algorithm in the present context; error estimates on ICES biomass estimates are only partial and incomplete. Another popular basis is variational data assimilation techniques (see, e.g. Barker et al., 2004), which explicitly balance model and observational uncertainty in a prescribed cost function. Again, incomplete characterization of uncertainty in model and ICES biomass estimates is an issue requiring extensive work. Implementing a Kalman or variational scheme in the present context will require extensive technical adaption, and since it is not our intention to present a paper on data assimilation per se, we will apply a simple nudging (aka Newtonian relaxation) scheme in the present work.

In this work we will assimilate regional spawning biomass (SSB_A) and regional total biomass (TSB_A), each corresponding to 4 pseudo observations each year. The model prediction

of SSB_A and TSB_A are given by Eqs. (A3) and (A4), respectively. These equations show that observations are not point samplings of the model state but correspond to regional sums over model states; this means that we need to have an assumption about error distribution within regions. Here we will apply the reasonable null assumption that the model error is proportional to model state variables. Further, since no direct observations of length distributions (at 1 January) are available in WGNSSK (2011), we associate model state errors with $N_{i\,\mathrm{a}}$ (thus not nudging $L_{i\,\mathrm{a}}$), which is supported by the presumption that the major error source in SPAM is unaccounted variability in predation mortality M. These two biologically reasonable assumptions makes the assimilation problem tractable as a rescaling of $N_{i\in A,\,\mathrm{a}}$ for each region A, since SSB_A and TSB_A depends linearly on $N_{i\in A,\,\mathrm{a}}$. Thus, in reanalysis mode, we apply the following Newtonian relaxation scheme after the forecast steps Eqs. (1)–(3):

$$N_{i\in A,\,\mathrm{a}} \leftarrow N_{i\in A,\,\mathrm{a}} + \kappa\,(\epsilon_A - 1)\,N_{i\in A,\,\mathrm{a}}, \tag{7}$$

$$\epsilon_A^{\mathrm{SSB}} = \frac{\mathrm{SSB}_A}{\sum_{i\in A,\,\mathrm{a}\geq 2} N_{i\,\mathrm{a}}\, w\,(L_{i\,\mathrm{a}})}, \tag{8}$$

and

$$\epsilon_A^{\mathrm{TSB}} = \frac{\mathrm{TSB}_A}{\sum_{i\in A,\,\mathrm{a}\geq 1} N_{i\,\mathrm{a}}\, w\,(L_{i\,\mathrm{a}})}, \tag{9}$$

where $\epsilon_A = \epsilon_A^{\mathrm{SSB}}$ or $\epsilon_A = \epsilon_A^{\mathrm{TSB}}$ or a linear combination thereof, if both SSB and TSB are being assimilated and $0 < \kappa < 1$ is the nudging pace, with $\kappa = 0$ being the pure hindcast mode limit and $\kappa = 1$ being the direct insertion mode limit, where model regional biomasses match ICES regional assessment. The nudging scheme above is not mass conserving; however, this is not a problem, because the sandeel stock is an open system internally governed by dissipative and creation processes, e.g. mortality, fishery and biomass growth.

2.6 Future climatic variability

The computational cost of a full decadal ensemble forecast of the lower trophic levels of the marine environment that is sufficiently constrained to quantify all the uncertainties involved in such a system is currently untractable in an operational system. The question is then what to use as environmental forcing when future predictions of stock development must be assessed, i.e. how should we generate future matrices $\mathbf{T}^{\mathrm{y}}$ needed for stock forecasting? In this paper we will only address the impact of future climatic variability – not climate change, which is a separate issue. We use a simple statistical extrapolation of the environmental forcing into the forecasting period, which requires no explicit projection of the environmental state, that would come at extremely high computational cost.

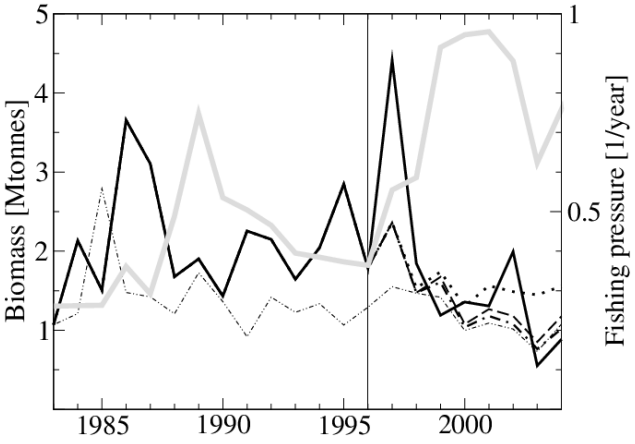

Fig. 4. Hindcast of the 1998–1999 sandeel stock regime shift, with full reanalysis for 1983–1996. The actual computed **T** matrices for 1983–2004 are imposed in all runs. Full thick line: actual stock biomass (left axis) from ICES stock assessment. Dotted line: 1996–2004 hindcast, freezing fishing pressure to 1996 level. Dashed line: 1996–2004 hindcast, imposing actual historic fishing pressure (higher than 1996 level). Dash-dotted line: 1996–2004 hindcast, imposing actual historic fishing pressure along with 20 % linear reduction in carrying capacity between 1997 and 2004. Dot-dot-dashed line: full-period 1983–2005 hindcast model run, applying actual historic fishing pressure. Full grey line (right axis): average actual historic fishing pressure, averaged over areas 1–3 for 1-yr-old sandeel.

For SPAM ensemble forecasts, simply, each member of the statistical ensembles each year independently drew a random member T of the set $\{\mathbf{T}^{\mathrm{y}}\}_{\mathrm{y}\in[1970;\,2004]}$ to generate the response envelope to interannual variability. This procedure is based on the assumption that the set $\{\mathbf{T}^{\mathrm{y}}\}_{\mathrm{y}\in[1970;\,2004]}$ spans the climatic variability and is supported by our previous finding that transport matrices $\mathbf{T}^{\mathrm{y}}$ of subsequent years have little correlation structure in the temporal variability, if any (Christensen et al., 2008).

2.7 Model validation

Validation of fish stock models is notoriously difficult because fish stock state can not be observed directly. Often one is most interested in the stock biomass, and for commercial stocks fish landings are the most important data source. However, there is no simple proportionality between biomass and landings, and data needs to be preprocessed under many assumptions and possibly combined with other data sources; consequently error estimates are difficult and incomplete. The most qualified estimates on fish stock biomasses come from fish stock assessments published by ICES (International Council for the Exploration of the Sea, see ices.dk), which combines fish landing data, survey data and many other data sources and continuously develops the applied methodologies. We will consider their estimates on fish stock biomasses as pseudo observations in the present work to parametrize

Table 1. SPAM model cost function "cf" (Eq. 10) on total biomass prediction ($\mathrm{TSB}^{\mathrm{y}} = \sum_{i,\,\mathrm{a}\geq 1} N^{\mathrm{y}}_{i,\,\mathrm{a}}\ w^{\mathrm{y}}_{i,\,\mathrm{a}}$) and total recruitment prediction ($R^{\mathrm{y}} = \sum_{ij} R^{\mathrm{y}}_{ij}$) with different data assimilation levels for 1983–2004. In all cases, the actual yearly calculated values of the transport ($\mathbf{T}^{\mathbf{y}}$) and assessed fishing mortality (F^{y}) was applied as forcing. In the column Nudging, the number in parenthesis refers to the value of κ giving highest skill.

		Skill		
Predicted property	Assimilated data	Hindcast ($\kappa = 0$)	Nudging (at optimal κ)	Direct insertion ($\kappa = 1$)
TSB	SSB	0.930	0.794 (0.68)	0.816
R	SSB	1.094	1.005 (1.00)	1.005
R	TSB	1.094	0.973 (0.90)	0.983

and validate the SPAM model. Our philosophy is to orient modelling toward available data sources and do the best possible job with this.

2.7.1 Model skill assessment

To assess the skill of the framework at various levels of data assimilation, we compared model output with results from ICES stock assessment WGNSSK (2011). The model skill for an output property X is quantified by the conventional cost function (Allen et al., 2007):

$$\mathrm{cf}(X) = \frac{1}{N}\sum_{q=1}^{N} \left| \frac{M_q^X - O_q^X}{\sigma\left(O^X\right)} \right|, \tag{10}$$

where M_q^X and O_q^X are the qth out of N matching pairs of model output and observation, respectively, on property X, and $\sigma(O^X)$ is the observed RMS on property X. We have applied the absolute value of each model residual to accentuate a potential time bias or model drift, if present. The performance level is conventionally ranked as cf < 1: very good, cf < 2: good, cf < 3: reasonable and cf > 3: poor (Radach and Moll, 2006).

In Table 1 we show the model skill for biomass (TSB) and recruitment (R) for the period 1983–2004. In all cases, with and without data assimilation, the model performs good or very good according to the cost function metric, Eq. (10), even in hindcast mode ($\kappa = 0$). In all cases, data assimilation ($\kappa > 0$) improves model skill a little, but not dramatically. In two cases, an intermediate value of nudging pace (κ) is optimal, whereas for recruitment R with data assimilation of SSB, the direct insertion limit ($\kappa = 1$) gives best skill; however, the variability with (κ) is not dramatic in this case. Figure 4 (dot-dot-dashed line) shows a full-period 1983–2005 hindcast model run, applying actual historic fishing pressure, compared to ICES stock assessment (full line). The figure shows that the model reproduces many characteristic fluctuations in the stock assessment data and basic statistical properties of the ICES stock assessment time series; a slight tendency to under estimate biomass in 1983–1996 is apparent – this is due to the fact that model carrying capacities are calibrated to the average biomass for period 1990–2011, which straddles the period with low stock abundance (see below).

2.7.2 Anatomy of the 1998–1999 regime shift

As mentioned in the introduction, North Sea sandeel stocks apparently underwent a regime shift around 1998–1999. This situation constitutes an interesting situation to validate the model's set-up. The most prevalent hypotheses for the triggering mechanism(s) are either overfishing or a shift in North Sea zooplankton composition. To delineate the causality behind this apparent regime shift, we ran hindcasts with different forcing scenarios as shown in Fig. 4, along with the actual stock development. The dotted line in Fig. 4 shows that no regime shift occurs if the fishing pressure is maintained at the 1996 level; if however, the actual historic fishing pressure is applied (dashed line), the model stock biomass displays a dip of quite similar magnitude as the actual historic stock biomass (as obtained from ICES stock assessment), and many characteristic fluctuations are reproduced even though the prominent biomass peak in 1997 is underestimated. The dashed line also constitutes a short-term comparison between model hindcast and actual data (full black line). The relative impact of a zooplankton quality change is modelled as a decline in the habitat carrying capacity C. The dash-dotted line in Fig. 4 shows the effect of a 20 % decline in habitat carrying capacity between 1997 and 2004 (relative to parametrized level) in conjunction with the historic fishing pressure. The effect is clearly smaller, and to obtain an effect similar to the fishing pressure increase, a 60–80 % decline in habitat carrying capacity between 1997 and 2004 is needed, a decline which is not reflected in observations to our knowledge; so, in summary, this exercise indicates that fishing pressure most likely triggered the apparent regime shift around 1998–1999, and the model is able to reproduce this effect. Finally, Fig. 4 clearly shows that the model reproduces the two-year auto correlation of the stock biomass, which is an emergent feature of the model. The fact that model performance in hindcast mode is quite decent reflects a fair mechanistic representation of biological processes in the coupled model framework, however for more operational purposes we recommend reanalysis mode to reduce model error further.

Since stock biomass assessments from ICES are used both for parametrization and validation, one may at first glance argue that there is a risk of circularity. However, parametrization of unknown biological variables, like the habitat carrying capacity C, are done using multidecadal averages of drivers (like T, F and M) in relation to multidecadal averages of local stock biomasses (B), thus giving time averages of biological variables like C. Validation, on the other hand is performed using drivers (T^{y}, F^{y}) for the actual year,

Table 2. Biological parameters in the SPAM model.

Parameter	Description	Value	Unit	Source
s	Larval minimum growth factor	0.67	–	Letcher et al. (1996)
L_0	Larval hatch length	6.3	mm	Jensen (2001)
L_∞	Adult length limit	218	mm	Macer (1966)
β	Growth exponent	0.768	–	Jensen (2001); Boulcott et al. (2007)
λ_0	Maximum growth prefactor	660	mm yr^{-1}	WGNSSK (2011)
ω	Relative growth variability	0.2	–	Jensen (2001)
w_∞	Adult weight limit	31.94	g	Macer (1966)
ϕ	Weight length exponent	3.068	–	Macer (1966)
Q_∞	Fecundity limit	12556	eggs	Macer (1966)
q	Fecundity length exponent	3.055	–	Macer (1966)
t_{larv}	Larval growth/drift period	8/52	yr	Jensen (2001)
t_{juv}	Juvenile growth period	12/52	yr	Jensen (2001)
t_{ps}	Post-settlement period	16/52	yr	Jensen (2001)
t_{agw}	Adult somatic growth period	10/52	yr	Jensen (2001)
t_{active}	Adult active period	20/52	yr	Jensen (2001)
t_{c}	Diagnostic fishing day (in active period)	1/52	yr	Diagnostic

Table 3. Inferred biotic/abiotic parameters in the SPAM model obtained from residual minimization.

Parameter	Description	Unit	Value in area i			
			1	2	3	4
α	Competition susceptibility	–	0.0425			
τ	Avg. life time of a hatched larvae	days	6.966			
C_i	Carrying capacity	t km^{-2}	2.36	2.04	2.54	2.08
ξ_i	Mortality weighting factor	–	1.18	1.13	1.00	0.84

compared to stock biomasses for the actual year (B^y), and therefore the validation is meaningful and tests the internal consistency and response properties of the stock model in this work, because the number of biological parameters is far less than the number of data points used for parametrization. Especially the regime shift situation above is a hindcast that tests the predictive capability of the stock model in this work, since the actual time varying forcing (the fishing history) is applied to test a characteristic known response.

3 Results

In this section we provide some examples of model output that illustrate how the forecasting system described above is able to address typical questions in relation to the scientific basis for spatial fish stock management and marine spatial planning. Conclusions for management should be based on statistical properties of stock dynamics rather than results for specific years, unless specific years are addressed, to avoid decisions potentially based on outliers in the stock dynamics. Each simulation starts with a spin-up period of 50 yr to relax age, size and spatial distribution of the fish stock. In all runs we start with a spin-up period where we apply area resolved time averages for the period 1990–2011 of stock drivers F, M, Z_0 and $\mathbf{T}$ (the latter at 10 km resolution); we refer to these as reference conditions. After this follows a reanalysis period (1983–2004), where TSB (WGNSSK, 2011) were assimilated with $\kappa = 1$, as described in Sect. 2.5 and applying year specific values of stock drivers F and $\mathbf{T}$. For all forecast ensemble runs 2004, the same initial conditions (state matrices $\mathbf{N}$ and $\mathbf{L}$) are applied to all ensembles members in the beginning of the forecast period, corresponding to system state at the end of the reanalysis period. In other words, ensembles were initialized by cloning the system state at the end of the reanalysis period.

3.1 Fish stock forecasts

In relation to fish stocks, short-term forecasts means 1–5 yr, whereas long-term forecasts means 10 yr.

Forcings were set to reference conditions in the forecasting period, apart from $\mathbf{T}$, which was assigned as described in Sect. 2.6. In Fig. 5 we show 20 yr forecasts based on ensemble runs for total stock biomass in WGNSSK areas $A = 1$–4 as defined in Fig. 1. The forecast in Fig. 5 were generated using ensembles with 100 members, initialized as described above. The purpose of these ensemble runs was to resolve

the climatic variability response envelope. Some features are very apparent: stock dynamics display a prominent two-year auto correlation, which is most clear in the forecast period 2004, especially for area 1, but also clearly visible in the assimilation period 1990–2004, where predation and fishing pressure fluctuates between years and masks the two-year auto correlation. The two-year auto correlation effect on the stock biomass is observed for the stock (Arnott and Ruxton, 2002; van Deurs et al., 2009) and is a population density effect which also is an emergent feature in the SPAM model parametrization. This population density effect comes from food competition between adult fish and offspring or cannibalism (on offspring) within the stock. It is also seen that the two-year auto correlation is not in phase between areas or ensembles, reflecting weak larval exchange between major regions.

An interesting property in relation to the validity of forecasts is the climatic envelope decorrelation timescale, i.e. the time it takes for interannual fluctuations to delete information of the stock past history, which sets an upper limit for medium/long-term predictions. This timescale is an intrinsic property of the stock dynamics model coupled to prevalent climatic forcing distribution $\mathbf{T}$. We have previously shown that transport matrices $\mathbf{T}^{\mathrm{y}}$ of subsequent years have little correlation structure in the temporal variability, if any (Christensen et al., 2008). If the stock starts with a certain biomass B_0, the distribution of biomasses will evolve as $P^t(B)$ with

$$P^t(B) \to \begin{cases} \delta(B - B_0), \; t = 0 \\ P^{\infty}(B), \quad t \to \infty \end{cases}, \tag{11}$$

where the attractor $P^{\infty}(B)$ is the is distribution of predicted biomasses in the far future (if the stock is forced with same climatic variability observed presently for a long time). In Fig. 5 we see that the attractors $P_A^{\infty}(B)$ are different for each area A, where area 2 has the broadest range. Also we note that area 4 is predicted to be prone to years of low biomass abundance, due to climatic variability.

The climatic envelope decorrelation timescale τ is then the speed at which $P^t(B)$ converges to $P^{\infty}(B)$. A rough estimator for τ is

$$\tau^{-1} \sim \frac{\frac{\mathrm{d}}{\mathrm{d}t}\mathrm{var}(B)_{t=0}}{\mathrm{var}(B)_{t=\infty}}. \tag{12}$$

For the simplest reference system that can be solved analytically, diffusion with an attractive point B_0,

$$\frac{\partial P}{\partial t} + \frac{\partial}{\partial B}\left(-D\frac{\partial P}{\partial B} - k(B - B_0)P\right) = 0, \tag{13}$$

the estimator Eq. (12) gives the exact timescale in the analytic solution, where diffusivity D and advection speed k are parameters.

The fact that transport matrices $\mathbf{T}^{\mathrm{y}}$ of subsequent years can be considered independent makes τ insensitive to which year we start. If the estimator Eq. (12) is applied to data in

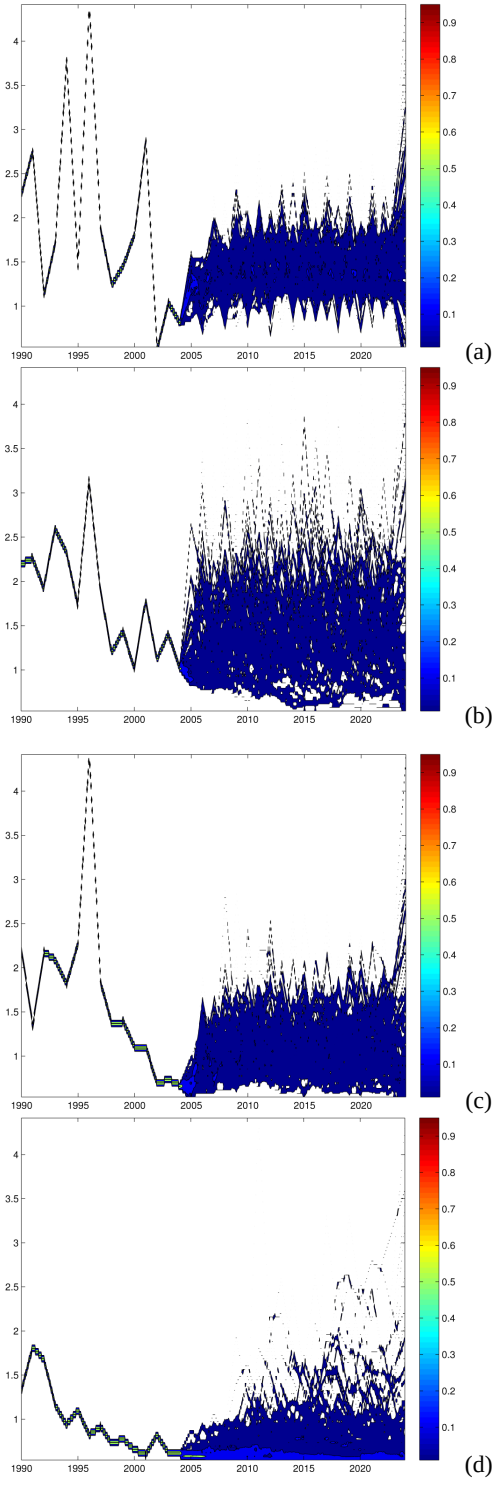

Fig. 5. 20 yr ensemble forecasts of biomass in area 1, 2, 3, and 4 following reanalysis run 1990–2004. The ensemble averages over climatic variability as represented by $\mathbf{T}$, by drawing deviates as described in Sect. 3.1: **(a)** WGNSSK area 1, **(b)** WGNSSK area 2, **(c)** WGNSSK area 3, **(d)** WGNSSK area 4.

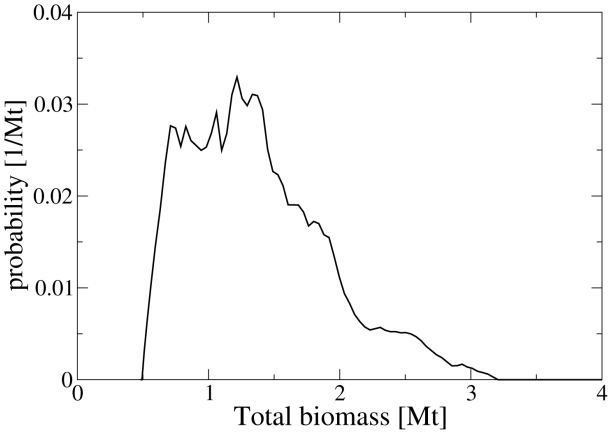

Fig. 6. Asymptotic total biomass attractor (distribution) for North Sea sandeel stocks $P^{\infty}_{\mathrm{NS}}(B)$ predicted by the SPAM model.

Fig. 5, we find that areas 1–4 have $\tau = (6, 2, 3, 10+)$ yr respectively, and the total biomass have $\tau = 5$ yr. Thus, unlike Lewy et al. (2004), we do not find that regional decorrelation timescales are consistently lower than basin-scale decorrelation, and one may speculate that their conclusion is related to their statistical approach. After this period, the system returns to a dynamic attractor $P^{\infty}_{A}(B)$ characteristic for each area. The asymptotic total biomass attractor for North Sea sandeel stocks $P^{\infty}_{\mathrm{NS}}(B)$ predicted by the SPAM model is shown in Fig. 6. It is important not to confuse the climatic envelope decorrelation timescale τ with climatic change timescales; the former addresses how the stock responds to climate variability, i.e. interannual climatic changes (considered stochastic) on short timescales not related to global warming (or other long-term timescales related to the Earth system). Finally we notice that the forecasts for 2004 predict stock returns to a higher average level, consistent with recent years' observations.

3.2 Spatial distributions and variability

An essential piece of information in spatial stock management is the spatial and temporal distribution and variability of the harvested biomass. In Fig. 7 we plot the biomass distribution (of 1 January) of contrasting years: 1996, 1997, and 2004. The contrasting years are chosen so that 1996 and 1997 are before the apparent stock regime shift (1998–1999) and 2004 after the apparent stock regime shift. The coupled framework was run in reanalysis mode for the period 1983 to 2004, with assimilation of SSB with $\kappa = 1$, applying actual forcings $\mathbf{T}^{y}$ and $\mathbf{F}^{y}$ for each year. We see that the biomass gets more concentrated in the Dogger bank region (left part of area 1 in Fig. 1) after the apparent stock regime shift, whereas it previously was more evenly distributed over the habitat network in Fig. 1. The subsequent years 1996 and 1997 were chosen to elucidate potential spatial patterns in the two-year autocorrelation in the stock biomass discussed

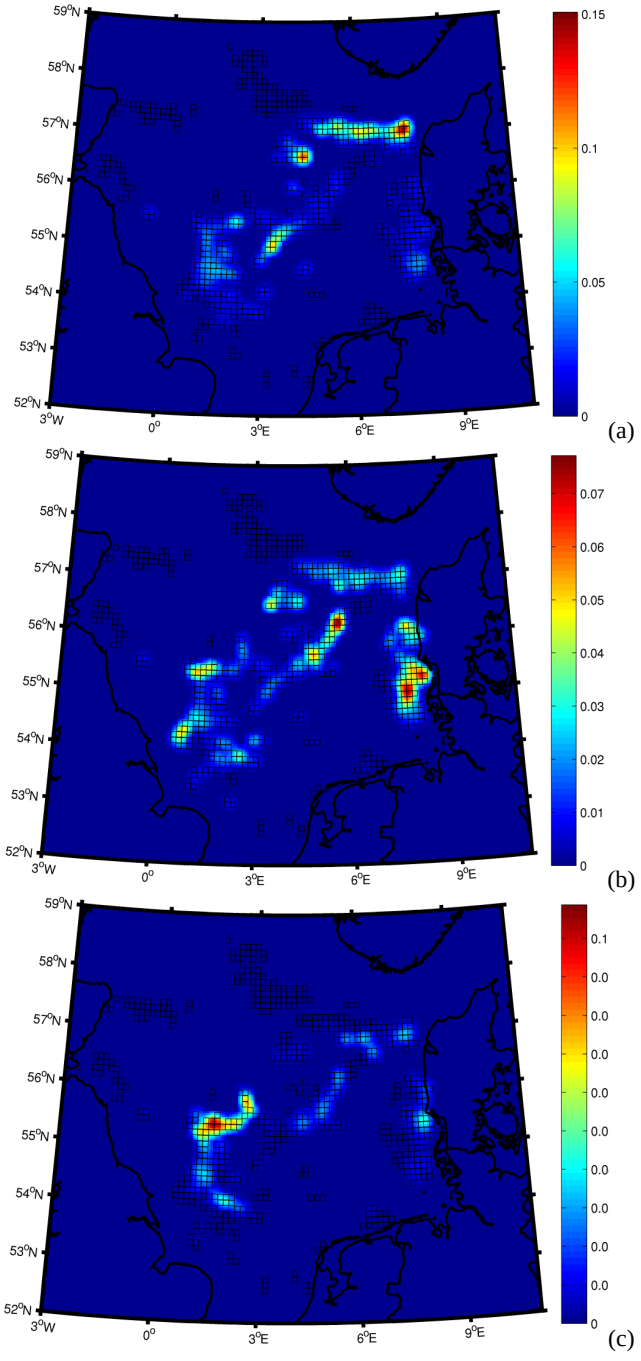

Fig. 7. Biomass distribution (in kt km^{-2}) for contrasting years. **(a)** 1996, **(b)** 1997, and **(c)** 2004. Small transparent boxes show suitable habitat areas (as 10×10 km boxes) for sandeel.

above in Sect. 3.1; here we see that "blinking" is not in phase between areas. We also see that there is significant spatial variability within each main area in Fig. 1, stressing the importance of spatially downscaling stock assessment results.

In Fig. 8 we show spatial distribution of stock recruitment intensity in 1997, based on a reanalysis for the period 1983 to 2004, with assimilation of SSB and application of year

specific values of **T** and F. Figure 8a shows recruitment intensity plotted by source, i.e. which habitats contribute most to the overall stock recruitment, and Fig. 8b shows areas of successful initial settlement of juveniles (regardless of where recruits came from). We see that there are significant differences between habitats that contribute and receive recruits on small scales, i.e. the stock dynamics on a small scale are strongly dependent on the exchange of larvae between nearby habitats. In a previous work (Christensen et al., 2008, 2007) we demonstrated that typical exchange distances are $\sim$ 50–100 km. Such source/sink analysis allows us to identify sensible areas (sources) and areas that can sustain heavy exploitation (sinks, which are automatically recolonized). Both spatial figures above indicate that the 10 km grid scale is sufficiently fine to resolve emergent spatial biomass variability scales, since the spatial variability pattern is not "zig-zag", but a lower scale appears to be around 20–30 km.

3.3 Local stock sensitivity

A way to access local stock sensitivity to harvesting is to plot and analyze the recruit-per-recruit derived maximum local fishing pressure ψ_i, Eq. (6). This is plotted in Fig. 9. Reference conditions were applied for M and Z_0, whereas actual historic values were applied for F and **T**. The field ψ_i was generated by solving Eq. (6) with the same fishing pressure for 1+ age groups and otherwise reference conditions; r_i in Eq. (4) was evaluated at $\mathbf{N} = 0$ (and $\mathbf{L}(\mathbf{N} = 0)$) which gives the upper limit for ψ_i, since mortality and growth processes are increasing and decreasing monotonously, respectively, with population density. Quite surprisingly, we see that some of the northern parts of the habitats are able to sustain the highest local fishing pressure, but on the other hand northern parts also have variable values for ψ_i: we see in Fig. 9 that quite a fraction of the north-eastern habitats have $\psi_i = 0$ due to the fact that $r_i < 1$ for any fishing pressure, suggesting that these areas are sinks. Another clear feature in Fig. 9 is that boundary habitats in the major areas have lower values for ψ_i than inner habitats: this is simply because of higher hydrographic loss of offspring for boundary habitats (offspring have lower probability of getting advected to a suitable settling habitat).

3.4 Stock management scenarios

A central issue in the scientific basis for stock management is at what fishing pressure does the stock give maximal catch and at which fishing pressure does the stock (risk) collapse. In Fig. 10 we show the predicted sustained catch for each WGNSSK area 1–4, along with the total catch, as function of spatial and temporal constant fishing pressure F for all 1+ age groups. The catches are 20 yr averages after a 50 yr relaxation period (to relax state variables, average out fluctuations and avoid stock depletion). Reference conditions applies for for M, Z_0 and **T**. The bars in Fig. 10 (only shown for the total catch) display the RMS on expected yearly catch that comes from inherent stock fluctuations generated by population density effects, indicating that large uncertainty is as-

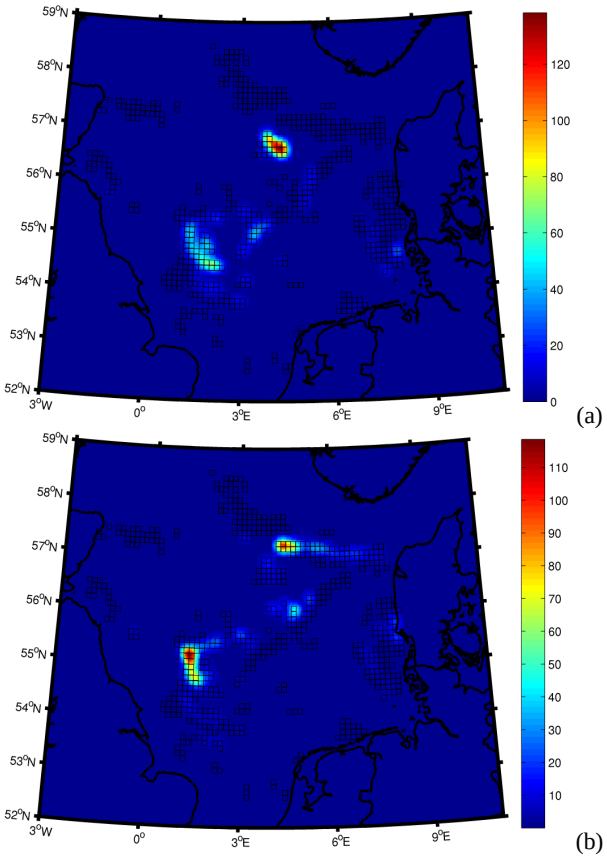

Fig. 8. Recruitment (million larvae per km^2 by end June) for 1997. **(a)** Recruitment intensity plotted by source and **(b)** recruitment intensity plotted by destination. Small transparent boxes show suitable habitat areas (as 10×10 km boxes) for sandeel.

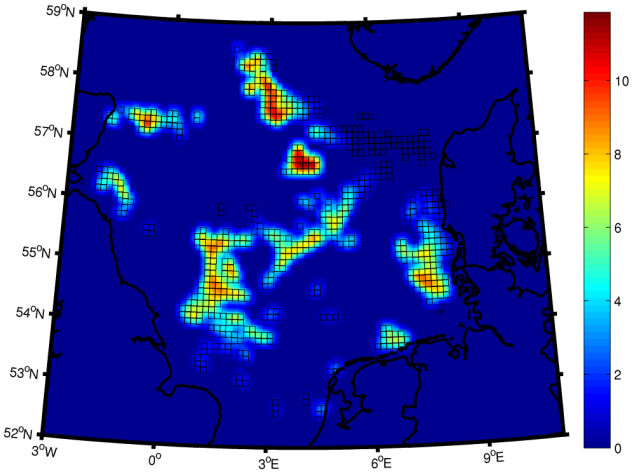

Fig. 9. Lineage analysis of maximal local fishing pressure ψ defined in Eq. (6). Small transparent boxes show suitable habitat areas (as 10×10 km boxes) for sandeel.

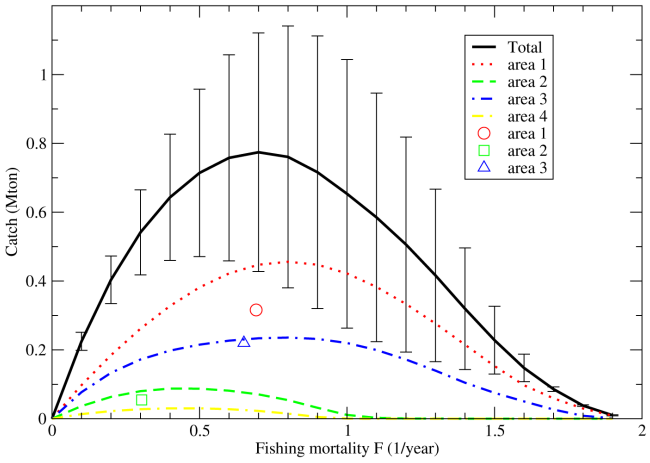

Fig. 10. MSY determination, applying same fishing mortality to all 1+ age groups. Error bars on total catch lines displays interannual total catch variability (RMS). Symbols show catch and fishing mortality (plainly averaged for the period 1990–2011) for each area.

sociated with determining stock maximum sustainable yield due to stock inherent dynamics and climatic variability, and that optimal long-term harvest is inherently associated with large interannual variability in catch. Symbols in Fig. 10 show actual historic catch and fishing mortality (plainly averaged for the period 1990–2011) for each area (no fishing mortality were available for area 4). We see that catches are slightly overestimated by the SPAM model in hindcast mode; however, the figure also suggests that the sandeel stocks are currently exploited close to the maximum sustainable yield (MSY) point, on average, in all areas 1–3, even though catch and fishing mortality displays large fluctuations in the period 1990–2011. We see that different areas have different optimal yield fishing pressures, ranging from $F \sim 0.4$ to $0.8\,\mathrm{yr}^{-1}$, with $F \sim 0.7\,\mathrm{yr}^{-1}$ as North Sea wide optimum. Stock collapses occur gradually, at different fishing pressures for different areas, between $F \sim 0.8\,\mathrm{yr}^{-1}$ (area 4) and $F \sim 2.0\,\mathrm{yr}^{-1}$ (areas 1, 3). This upper limit is consistent with the local estimates based on recruit-per-recruit analysis, see Fig. 9. We see that the route of stock collapse is gradual when increasing fishing pressures: the stock concentrates in the most productive habitats, while extinguishing in lesser productive habitats; this pattern need not be generic to other sedentary fish species. For $F > F_{\mathrm{MSY}}$, catch fluctuations increase, until close to stock collapse, where fluctuations become very small; this is due to the fact that stock density effects disappear, because the stock does not utilize the habitat carrying capacity. Another way to appreciate this comes from the observation that fish stock models essentially map to a discrete logistic map (see, e.g. Murray, 2002): increasing F drives fish stock models reversely through bifurcation cascades, eventually collapsing the stock; the decrease in catch fluctuations for decreasing F comes along because catch is the product of F and biomass, which saturates at lower F.

4 Discussion

The forecasting system presented in this paper consisted of three major building blocks: the Eulerian POLCOMS system for physics, the Lagrangian model SLAM for early life stages, and SPAM, the discrete box model for spatial fish population dynamics. All these three model systems are developed independently in different coding languages and are mathematically very different and address different timescales. These aspects stress the importance of well-defined interfaces, e.g. POLCOMS and SLAM are coupled by exchanging daily/sub-daily time frames of full three-dimensional oceanographic data, whereas the coupling from SLAM to SPAM (and POLCOMS to SPAM) is via biologically meaningful annual index matrices like **T** (and **S** and **Q**) produced by SLAM using oceanographic data from POLCOMS. The strength of this is that it allows independent improvements of all components: POLCOMS, SLAM and SPAM.

The three models can in principle run in online mode, exchanging data via files (or data pointers), or offline, exchanging data via files only. Times series for full three-dimensional oceanographic data are relatively big (0.1–10 TB) for 10–50 yr needed for spanning climatic variability, but this becomes feasible with present day storing capacity and data exchange rates. Annual index matrices, like **T**, require negligible storage once computed. The offline mode is definitely an advantage during interactive development, iterative calibration runs and for the statistical extrapolation of past states into the future applied in this study. Online coupling may be relevant for production runs, but, as mentioned above, the three model components are not load balanced. However, online mode would become necessary in order to include the grazing feedback of the fish/fish larvae on the plankton biomass of the lower trophic level model, if zooplankton grazing from fish/fish larvae is included. The relative model load is set by the integration time step, which is smallest for POLCOMS (on the order of seconds for the external mode and around 15 min for the internal mode), in the middle for SLAM (30 min) and largest for SPAM ($\sim$ seasons–1 yr). Consequently, it becomes attractive for iterative fish stock simulations (e.g. parameter calibration runs over same time window) to run offline, whereas the addition of the SLAM/SPAM component has negligible impact on the POLCOMS system in terms of computational resources, unless the SPAM simulation includes an excessive number of ensembles.

We used the fish species sandeel in the North Sea as a case study to illustrate our forecasting system, however it is possible with little or modest effort to adapt the system to cover other habitat-bound fish species as well. The SLAM model is a set-up within the IBMlib framework to handle North Sea sandeel stocks; the IBMlib framework can handle any early life stage with suitable adaptation for hatching, growth, active movement and adult transition, and the generality of

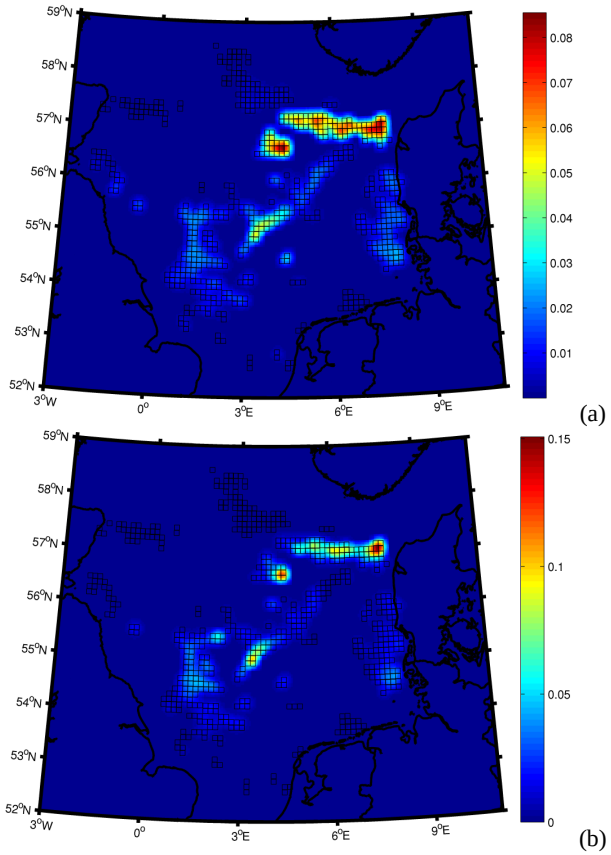

Fig. 11. Biomass distribution (in kt km^{-2}) for 1996 **(a)** with post-settlement migration (Eq. A14) and **(b)** without post-settlement migration.

IBMlib is demonstrated by a growing base of case studies using IBMlib beyond sandeel, e.g. herring (Fassler et al., 2011), cod (Beyer et al., 2012), sprat (Christensen et al., in prep), mackerel (Jansen et al., 2012), blue whiting (Payne et al., 2012), as well as and generic trait-based studies (Mariani et al., 2013). The IBMlib framework has interfaces to numerous physical data sets. In another region, the IBMlib framework is easily coupled to another physical model as illustrated by the references above. The SPAM core model Eqs. (1)–(3) is fairly general, expressed in terms of generic life cycle events, and applies to most habitat-bound species. Of course, when addressing another species, minor or modest adaptations should be done. A new habitat map should be provided; biological parameters should be adjusted and particular processes, like the density dependence, should be reparametrized. The most significant limitation in the core model Eqs. (1)–(3) is stocks being habitat-bound (apart from the pelagic phase). Limited migratory behaviour is fairly straightforward to implement and is illustrated in Appendix A2, and involving a migration matrix, applied in addition to Eqs. (1)–(3) in each time step. Of course, in the case of directional movement, it is a major challenge to parametrize and construct realistic and robust parametrizations of the variability in the migration in relation to the environment (and model state variables), as noted in the introduction. Depending on the desired accuracy and complexity of biological modelling, other minor extensions are feasible, like intra-seasonal time steps and alternative synchronizations of life history events. In summary, the SPAM is the model component requiring relatively most extensions and adaptations to encompass other fish species by the forecasting system presented in this paper.

When parametrizing the fish stock model component SPAM, we have not imposed a stable equilibrium state, but rather included the limit cycle (attractor) of the biological model which is consistent with biological observations, displaying negative autocorrelation of biomass between subsequent years. This of course poses extra challenges when parametrizing a model, but this has been accomplished by focusing on statistical properties of the limit cycle of the biological model, as elaborated in Appendix A.

Facing that the computational cost of a full decadal ensemble forecast of the lower trophic levels of the marine environment requires excessive computer resources, we have applied a simple "pick-a-random-past-year" scheme for future climate forcing that reproduces statistical properties of a historical time series by construction; however alternative schemes to generate synthetic $\mathbf{T}$ time series are conceivable, e.g. convex interpolation in a historic time series like

$$\mathbf{T}^z = \sum_y s_y^z \mathbf{T}^y, \tag{14}$$

where $0 < s^z < 1$ is a random vector with $\sum_y s_y^z = 1$. This sampling scheme has smaller variance $< \mathbf{T} \times \mathbf{T} > - \bar{\mathbf{T}} \times \bar{\mathbf{T}}$ than the random-year sampling scheme applied in this paper. Also, this scheme may blur a potential covariation and clustering in the historical set $\mathbf{T}^y$. Alternatively, principal-component correlation with teleconnection indices (Barnston and Livezey, 1987), like NAO, could be applied. We believe that a scheme for generating a synthetic $\mathbf{T}$ time series should satisfy certain minimal requirements like $T > 0$ and reproducing basic statistical properties of a $\mathbf{T}^y$.

We found that the decorrelation time τ of biomass dynamics due to stochastic climatic variability is of order 2–6 yr, with some variations between areas in the modelled region; this is the time it takes for random kicks from the climatic variability to wash out the past biological state of the fish stock; this time frame is somewhat encouraging in that it allows for some short to medium timescale economical planning. When the time horizon exceeds ~ 6 yr, the principal model output is the asymptotic probability distributions (attractors) of the system properties, e.g. $P^\infty(B)$ the probability distribution of biomasses in the far future. These attractors are also very useful for management scenarios; they limit the ignorance of the future and provide an average trend as well as variability on the stock state when subjected to alternative management scenarios.

The complexity of life processes increases as one moves up the trophic chain, and therefore many assumptions have to be made for early life stages (the SLAM model) and adult fish (the SPAM model).

In calculating transport indices **T** in the SLAM model, we have made certain biological assumptions, e.g. a fixed spawning day (20 February), where offspring begins the pelagic transport. In our previous work (Christensen et al., 2008), we examined the the effect of this and other biological approximations, like the settlement dynamics, on the calculated transport indices **T**. At regional scale, we found relative transport probabilities to be rather robust toward parameter perturbations, however differences were found. Currently, a fixed average spawning day represents "best knowledge", because no data exist to relate a spawning distribution to environmental cues. Of course, this contributes to the overall envelope of uncertainty of the model predictions. In the SLAM model, for example, active motion of larvae has not been included, as well as grazing feedback on zooplankton from sandeel larvae. The latter is partially justified by the fact that sandeel larvae and adults on average only constitute a fraction of the zooplankton grazing biomass, even though locally sandeel may dominate the zooplankton grazing (A. Rindorf, personal communication, 2011). This isolated grazing feedback from sandeel on zooplankton is partially represented by the density dependence of S, see Eq. (A12). From a parallel study (Mariani et al, 2013), we know that active vertical motion of larvae in the North Sea have some, but not dramatic, impact on horizontal transport for typical variability in vertical motion patterns; however, presently biological models on sub-daily vertical migration are uncertain and still at a research stage. This and other sources of biological uncertainty adds some basic uncertainty to the calculation of transport matrices and improving this is a topic in future research.

A potential way to assess impact on population dynamics from uncertainty in calculated transport indices **T** for a given year (or as part of a scenario) is to compute the distribution $p(\mathbf{T})$ of transport matrices over the distribution of biological parameters associated with the larval pelagic phase; by subjecting the distribution $p(\mathbf{T})$ to principal component analysis, it is possible to sample the intra-year range of **T** of generated ensemble runs, similarly to the future climatic response envelopes in Sect. 3.1. Effectively, this will lower the forecast decorrelation timescales we established earlier.

In the recent years several studies, e.g. Daewel et al. (2008); Hufnagl and Peck (2011); Gurkan et al. (2012, 2013), on models for predicting larval survival **S** and growth in relation to the biogeochemical environment have been published, based on the generic model in Letcher et al. (1996). These bioenergetic models typically contain 60+ parameters, most of which can only be guessed or taken from other species. Thus, even though they provide interesting insight into biology, their quantitative skills are uncertain, especially in that they possess higher predictive skill than simple temperature-driven models, as applied in our study. Indeed the predictions of these bioenergetic models are strongly dependent on zooplankton size spectrum, which are seasonally varying. Most biogeochemical models, e.g. ERSEM (Edwards et al., 2012), do not output zooplankton size spectra, but only vaguely defined bulk micro- and macrozooplankton biomasses, so the size spectrum must be reverse engineered, introducing yet further assumptions, even though some attempts are emerging to include size- and stage structure of zooplankton (Maar et al., 2013). Further, the bloom dynamics of zooplankton in biogeochemical models do not match observations sufficiently well yet, even though progress is good. Finally, it has been hypothesized that the most important bottom-up impact on North Sea larvae comes from a taxonomic shift in the zooplankton community structure, a feature which is not modelled in present biogeochemical models. In summary, bioenergetic models for **S** are still at research level and not on operational level. Anyway, all these uncertainties are absorbed in the product of **T** and **S** in the integrated framework, and decreasing uncertainties is a topic in future research. However, such efforts may potentially increase forecast decorrelation timescales toward the limit set by climatic variability.

In the SPAM model the major short comings are the lack of spatial and temporal heterogeneity of predation pressure on the fish stock. This will decrease the decorrelation timescales τ found in Sect. 3.1. In the present paper, a spatial and temporal average predation pressure was applied, as available from stock assessment work (WGNSSK, 2011). In the future, it is conceivable that temporal variability can be modelled from multispecies stock assessment time series, in conjunction with predator–prey interaction matrices. For the present case study, North Sea sandeels, data did not currently support a plausible parametrization of growth response to zooplankton variability. Additionally, the habitat carrying capacity did not include temporal variability, due to lack of data. The current parametrization however did not indicate very strong gradients in habitat carrying capacity in the North Sea for sandeel (see Appendix A), but spatially coherent interannual fluctuations are quite likely. Finally post-settlement adult migration was not included; adult sandeel are believed to display only small scale migration ($\ll 28$ km) (Jensen et al., 2011), triggered by daily feeding cycles. In Appendix A we show for high resolution set-ups like the one in the present paper that this will create a minor spill-over effects between adjacent habitats, but will not affect results on mesoscale, ~ 50 km.

5 Conclusions

We have presented an integrated forecasting system describing a single fish species, which is based on process-oriented simulation of ecosystem dynamics, from physics to fish, and presented a few illustrative examples of using our forecasting framework on questions relevant to management of fish stock, e.g. providing short-term forecasts including the effects of climatic variability and downscaling regional scale

stock assessments. We have demonstrated that the integrated forecasting system is a flexible tool for assessing effects of alternative fishing scenarios and providing biological insight into stock dynamics. The spatial explicit nature of the forecasting system allows for very rich and highly policy relevant output, e.g. warning signs of over fishing and imminent stock collapse from spatial signatures of how habitats are depleted, as well as risk of stochastic extinction of local fish stocks. Even though fish stock assessment results are associated with significant uncertainty, model skill benchmarks in this paper indicate that numerical representation of biological oceanographic processes underlying recruitment still needs to be improved, even though model skill currently was found to be quite good.

Appendix A

SPAM parametrization

In this Appendix we briefly summarize the parametrization of the biological processes in the SPAM model. Most parameters and process representations of the high resolution (10 km) set-up are the same as in the previous regional scale ($\sim$ 100 km) set-up, see Christensen et al. (2009), where a more elaborate derivation and model discussion can be found, along with a parameter sensitivity test. We adhere to the notation established there. In the following, i designates habitat cell in question, "y" year for time varying properties, and "a" age of a cohort.

A1 Model equations

The local population density index ρ is defined per habitat cell as

$$\rho_i^{\mathrm{y}} = \frac{B_i^{\mathrm{y}}}{C_i^{\mathrm{y}}} = \frac{\sum_{\mathrm{a}>0} N_i^{\mathrm{y}} w_{i,\mathrm{a}}^{\mathrm{y}}}{C_i}, \tag{A1}$$

where B_i^{y} and C_i^{y} are the local biomass and carrying capacity, respectively. In the present set-up, $C_i^{\mathrm{y}} = C_i$ is time independent. ρ regulates growth and survival in the model; note that C_i^{y} is a scale not an upper limit. $w_{i,\mathrm{a}}^{\mathrm{y}}$ is the dynamic weight-at-age. For length-based processes, a fixed weight–length key is applied:

$$w = w_\infty \left(\frac{L}{L_\infty}\right)^{\phi}. \tag{A2}$$

Thereby, also the regional spawning biomass (of age ≥ 2) SSB and the regional total adult biomass (of age ≥ 1) TSB become available:

$$\mathrm{SSB}_A = \sum_{i\in A,\,\mathrm{a}\geq 2} N_{i\mathrm{a}} w(L_{i\mathrm{a}}) \quad \text{and} \tag{A3}$$

$$\mathrm{TSB}_A = \sum_{i\in A,\,\mathrm{a}\geq 1} N_{i\mathrm{a}} w(L_{i\mathrm{a}}), \tag{A4}$$

where A refers to a region in Fig. 1. Larval/adult growth is controlled by the growth equation:

$$\frac{\mathrm{d}L}{\mathrm{d}t} = \lambda(\rho)\left(\left(\frac{L}{L_\infty}\right)^{1-\beta} - \frac{L}{L_\infty}\right), \tag{A5}$$

which is integrated analytically over the non-hibernation periods to give g_i in Eq. (2). The local growth potential is parametrized as

$$\lambda(\rho) = \lambda_0 \frac{1+\rho}{1+\rho+\alpha\rho^2}, \tag{A6}$$

where α is the competition susceptibility. For larvae transported between habitats i and j, the geometric average $\rho_{ij} = \frac{1}{2}(\rho_i + \rho_j)$ is applied in Eq. (A6).

It has also been tested by multivariate analysis whether the growth prefactor λ_0 exhibited correlation with ocean temperature and zooplankton (food) variability, since cohort growth time series can be inferred from available catch data (WGNSSK, 2011). Zooplankton 4D fields were extracted from the biogeochemical model ERSEM in the operational POLCOMS-ERSEM system (Butenschön et al., 2012; Edwards et al., 2012), with same physics set-up as described in Sect. 2.1. We generated an annual index of habitat temperature by averaging temperature from POLCOMS vertically and horizontally over habitats in Fig. 1 for the growth season 20 February–1 June of each year. For zooplankton (food) we made an annual index by horizontally averaging the vertical peak concentration of micro- and mesozooplankton output from ERSEM over habitats in Fig. 1 for the growth season 20 February–1 June of each year. We found no correlation between cohort adult growth and the habitat temperature index. Quite surprisingly however, zooplankton correlated negatively with cohort growth, i.e. more food implied less somatic growth. The negative correlation was rather weak (only able to explain 5 % of the growth variation), yet statistically significant. This is quite counter-intuitive, and until a biological understanding of this unexpected correlation is available, we think it is best for the realism of the overall set-up not to include this correlation. Anyway, the correlation is far below the overall uncertainty of the framework, which is another reason for not including it in the present version. The current hypothesis is that zooplankton quality is negatively correlated to zooplankton biomass, however the current version of ERSEM available for this work does not resolve zooplankton biomass into species. Alternatively, it may also be an indirect ecosystem effect, or some other biological mechanism.

Current observations only support a simple standard parametrization of fecundity as

$$Q_{i,\mathrm{a}} = Q_\infty \left(\frac{L}{L_\infty}\right)^{q} \mu(a-2), \tag{A7}$$

where a is the fish age and μ is the step function, i.e. fecundity variability is correlated to growth variability in the

model. For sandeel larvae, models describing the effect of zooplankton variability on larval growth and survival are still at the research level and need further validation. This issue is elaborated in the discussion of this paper. Therefore, a simplified model is applied where the larval conditional (given transport) survival S is the product of the predation avoidance S_p and starvation avoidance S_s. The former is parametrized as

$$S_\mathrm{p} = e^{-M_\mathrm{pl} t_\mathrm{larv}}, \tag{A8}$$

where t_larv is the duration of the larval drift phase.

Here we note that in the present SPAM set-up the value applied for t_larv is a characteristic average value, not the actual pelagic period distributions calculated in SLAM; on average (by parametrization), these timescales are similar and the variability of t_larv from SLAM is less than the spatio-temporal variability of M_pl, which is the average larval predation risk.

Currently no sub-model is available to assess the variability of M_pl, and therefore M_pl is estimated from from size spectrum theory as

$$M_\mathrm{pl} = \frac{\eta \xi_i}{\tau}, \tag{A9}$$

where τ is the expected life time of a newly hatched larvae before it gets eaten, on average. The prefactor η is slightly species specific and depends on average growth speed and length-at-settlement. ξ_i is an area specific weighting factor of order unity (explained below).

$$\eta = \frac{\tau}{t_\mathrm{larv}} \int_0^{t_\mathrm{larv}} M_\mathrm{p}(t) \quad \text{and} \tag{A10}$$

$$\eta = \frac{1}{\frac{L_\mathrm{m}}{L_0} - 1} \frac{1}{1-\nu} \left(\left(\frac{L_\mathrm{m}}{L_0} \right)^{1-\nu} - 1 \right), \tag{A11}$$

which for sandeel gives $\eta \sim 0.403$, where $-\nu \sim -3/4$ is the standard length–mortality scaling (West et al., 2001). Starvation avoidance S_s is parametrized as

$$S_\mathrm{s}(\rho) = \frac{1}{2} + \frac{1}{2} \mathrm{erf} \left(\frac{1 - \frac{\lambda_0}{\lambda(\rho)}}{\omega} \right). \tag{A12}$$

Finally, stock catches are estimated from the narrow-season limit as

$$Y^\mathrm{y}_{i,\mathrm{a}} = N^\mathrm{y}_{i,\mathrm{a}} \left(1 - e^{\left(-Z_0 - M^\mathrm{y}_{i,\mathrm{a}} \right) t_\mathrm{c}} \right) \left(1 - e^{-F^\mathrm{y}_{i,\mathrm{a}}} \right) w^\mathrm{y}_{i,\mathrm{a}}(t_\mathrm{c}), \tag{A13}$$

where t_c is duration from the end of hibernation to the middle of the (narrow) catch season. $w^\mathrm{y}_{i,\mathrm{a}}(t_\mathrm{c})$ is the average weight at catch, computed from Eqs. (A5) and (A2).

A2 Post-settlement adult migration

Adult sandeel are believed to display only small-scale migration (<28 km) (Jensen et al., 2011), triggered by daily feeding cycles. In the SPAM model, post-settlement migration is represented by

$$N^{\mathrm{y}+1}_{i,\mathrm{a}} = \sum_j A_{ij} N^{\mathrm{y}+1}_{j,\mathrm{a}}, \tag{A14}$$

evaluated after Eqs. (1)–(3). A_{ij} represents annually accumulated migration, which is a product of independent daily migrations A^1_{ij} between adjacent habitats:

$$\mathbf{A} = \left(\mathbf{A^1} \right)^n, \tag{A15}$$

where $n = 365\, T_\mathrm{a}$ is the number of feeding days during a season. Expressing $\mathbf{A}$ as a matrix product rather than just distance-dependent matrix elements makes a difference close to the edges and for stepping-stone habitats. The daily transition probability t between adjacent habitats in $\mathbf{A^1}$ is found from

$$t = \frac{D}{\Delta^2 365} \quad \text{and} \tag{A16}$$

$$D = \frac{R^2}{2T_\mathrm{a}}, \tag{A17}$$

where the post-settlement annual migration scale $R \sim 28$ km (Jensen et al., 2011) is applied, $T_\mathrm{a} = 140/365$, and habitat size $\Delta = 10$ km. The effect of Eq. (A14) is to create minor spill-over effects between adjacent habitats, which is illustrated in Fig. 11, where reference conditions apply for M, Z_0 and $\mathbf{T}$. Therefore adult migration has not been included in the main body of the paper for simplicity. Here $\mathbf{A}$ was parametrized for the daily loitering mechanism of adult sandeel; for other species $\mathbf{A}$ may further include directional movement and density-regulated migration.

A3 Biological parameters

Since SPAM is a process-oriented model, many parameters are available from the literature; these parameters along with references are provided in Table 2. The background mortality Z_0 (other sources) was included in the predation mortality because it was not separable from the predation mortality.

A4 Reference conditions

Reference conditions refer to average values (WGNSSK, 2011) (over the reference period 1990–2011) applied to stock drivers: predation mortality $\bar{M}_{i,\mathrm{a}}$ and fishing mortality $\bar{F}_{i,\mathrm{a}}$. For predation mortality, only a North Sea average value was provided (WGNSSK, 2011), $\bar{M}_\mathrm{a}$, and the area-specific predation mortality was constructed as

$$M^\mathrm{y}_{i,\mathrm{a}} = \bar{M}_\mathrm{a} \xi_i \tag{A18}$$

so that larval and adult predation risk are correlated (reflecting spatial heterogeneity in density of predators). Similarly, under reference conditions, $\mathbf{T}$ was averaged over the reference period 1990–2011, $\bar{\mathbf{T}} = \langle \mathbf{T}^{y} \rangle_{y \in [1990-2011]}$; reference carrying capacity was set as outlined below.

A5 Inferred biotic/abiotic parameters

For the remaining model parameters, there were insufficient empirical bases for direct parameter estimation, and these parameters are estimated from SPAM model output by minimizing a residual of remaining observations to generate a time-independent estimate of models parameters. These parameters are mostly area weighting factors representing spatial heterogeneity, and these are given in Table 3. No spatial heterogeneity were allowed for α and τ to avoid overparametrization. We also see that spatial variability of C_i and ξ_i are in a sensible regime, creating confidence to the robustness of the parametrization. The residual used to infer α, τ, C_i, and ξ_i was the sum of residuals for $\langle \mathrm{TSB} \rangle_i$, RMS ($\mathrm{TSB}_i$) and average growth for the reference period 1990–2011 in each area as provided by WGNSSK (2011).

Acknowledgements. We acknowledge financial support from the EU FP7 projects MyOcean (project no: FP7-SPACE-2007-1), MEECE (contract no: 212085) and OpEc (contract no: 283291) to conduct the present work. One of us (ZG) also acknowledges financial support from The Danish Strategic Research Council, within the project SUNFISH. AC is grateful for critical proof reading of the manuscript by Henrik Mosegaard, who also shared his insight into sandeel stock dynamics with us, and AC also acknowledges stimulating discussions with Uffe H. Thygesen about synthetic time series.

Edited by: P. Brasseur

References

Alheit, J.: Consequences of regime shifts for marine food webs, Int. J. Earth. Sci., 98, 261–268, doi:10.1007/s00531-007-0232-9, 2009.

Allen, J. I., Blackford, J. C., Holt, J., Proctor, R., Ashworth, M., and Siddorn, J.: A highly spatially resolved ecosystem model for the North West European Continental Shelf, Sarsia, 86, 423–440, 2001.

Allen, J. I., Holt, J. T., Blackford, J., and Proctor, R.: Error quantification of a high-resolution coupled hydrodynamic-ecosystem coastal-ocean model: Part 2, J. Marine Syst., 68, 381–404, doi:10.1016/j.jmarsys.2007.01.005, 2007.

Arnott, S. A. and Ruxton, G. D.: Sandeel recruitment in the North Sea: demographic, climatic and trophic effects, Mar. Ecol.-Prog. Ser., 238, 199–210, 2002.

Barker, D. M., Huang, W., Guo, Y. R., Bourgeois, A. J., and Xiao, Q. N.: A three-dimensional variational data assimilation system for MM5: Implementation and initial results, Mon. Weath. Rev., 132, 897–914, 2004.

Barnston, A. G. and Livezey, R. E.: Classification, seasonality and persistence of low-frequency atmospheric circulation patterns, Mon. Weather Rev., 115, 1083–1126, 1987.

Beaugrand, G., Reid, P., Ibanez, F., Lindley, J., and Edwards, M.: Reorganization of North Atlantic marine copepod biodiversity and climate, Science, 296, 1692–1694, doi:10.1126/science.1071329, 2002.

Beaugrand, G., Brander, K., Lindley, J., Souissi, S., and Reid, P.: Plankton effect on cod recruitment in the North Sea, Nature, 426, 661–664, doi:10.1038/nature02164, 2003.

Beyer, J., Pedersen, E. M., Wieland, K., Andersen, N. G., Andersen, B. S., Hansen, J. H., Hussy, K., Kristensen, K., Madsen, N., Mariani, P., and Stage, B.: Optimization of fisheries resource exploitation in the Skagerrak (Oskar), DTU Aqua report, 239, 2012.

Boulcott, P., Wright, P. J., Gibb, F. M., Jensen, H., and Gibb, I. M.: Regional variation in maturation of sandeels in the North Sea, Ices J. Mar. Sci., 64, 369–376, doi:10.1093/icesjms/fsl033, 2007.

Brasseur, P., Gruber, N., Barciela, R., Brander, K., Doron, M., El Moussaoui, A., Hobday, A. J., Huret, M., Kremeur, A.-S., Lehodey, P., Matear, R., Moulin, C., Murtugudde, R., Senina, I., and Svendsen, E.: Integrating biogeochemistry and ecology into ocean data assimilation systems, Oceanogr., 22, 192–201, 2009.

Butenschön, M., Holt, J., Artioli, Y., Wakelin, S., Saux Picart, S., de Mora, L., Blackford, J., and Allen, J.: Dominant Temporal and Spatial Features of the Intra-annual Phytoplankton Dynamics on the North-West European Shelf: A modelling study, Ocean Sci. Discuss., in preparation, 2013.

Carpenter, S.: Ecological futures: Building an ecology of the long now, Ecology, 83, 2069–2083, doi:10.2307/3072038, 2002.

Chen, D. and Ware, D.: A neural network model for forecasting fish stock recruitment, Can. J. Fish. Aquat. Sci., 56, 2385–2396, doi:10.1139/cjfas-56-12-2385, 1999.

Christensen, A., Daewel, U., Jensen, H., Mosegaard, H., St. John, M., and Schrum, C.: Hydrodynamic backtracking of fish larvae by individual-based modelling, Mar. Ecol.-Prog. Ser., 347, 221–232, 2007.

Christensen, A., Jensen, H., Mosegaard, M., M., S. J., and Schrum, C.: Sandeel (Ammodytes marinus) larval transport patterns in North Sea from an individual-based hydrodynamic egg and larval model, Can. J. Fish. Aquat. Sci., 65, 1498–1511, doi:10.1139/F08-073, 2008.

Christensen, A., Jensen, H., and Mosegaard, M.: Spatially resolved fish population analysis for designing MPAs: influence on inside and neighbouring habitats, Ices J. Mar. Sci., 66, 56–63, 2009.

Daewel, U., Peck, M. A., Alekseeva, I., John, S., M. A., Kahn, W., and Schrum, C.: Coupling ecosystem and individual-based models to simulate the influence of climate variability on potential growth and survival of larval fish in the North Sea, Fish. Ocean., 17, 333–351, 2008.

Edwards, K. P., Barciela, R., and Butenschön, M.: Validation of the NEMO-ERSEM operational ecosystem model for the North West European Continental Shelf, Ocean Sci. Discuss., 9, 745–786, doi:10.5194/osd-9-745-2012, 2012

Fassler, S. M. M., Payne, M. R., Brunel, T., and Dickey-Collas, M.: Does larval mortality influence population dynamics?, An analysis of North Sea herring (Clupea harengus) time series, Fish. Oceanogr., 20, 530–543, 2011.

Fulton, E. A: Approaches to end to end ecosystem models, J. Mar. Sys., 81, 171–183, 2010.

Fulton, E., Smith, A., and Johnson, C.: Effect of complexity on marine ecosystem models, Mar. Ecol.-Prog. Ser., 253, 1–16, doi:10.3354/meps253001, 2003.

Fulton, E. A., Link, J. S., Kaplan, I. C., Savina-Rolland, M., Johnson, P., Ainsworth, C., Horne, P., Gorton, R., Gamble, R. J., Smith, A. D. M., and Smith, D. C.: Lessons in modelling and management of marine ecosystems: the Atlantis experience, Fish Fish., 12, 171–188, doi:10.1111/j.1467-2979.2011.00412.x, 2011.

Gallego, A., North, E. W., and Petitgas, P.: Introduction: status and future of modelling physical-biological interactions during the early life of fishes, Mar. Ecol.-Prog. Ser., 345, 121–126, 2007.

Grandgeorge, M., Wanless, S., Dunn, T. E., Maumy, M., Beaugrand, G., and Gremillet, D.: Resilience of the British and Irish seabird Community in the twentieth century, Aquat. Biol., 4, 187–199, doi:10.3354/ab00095, 2008.

Gurkan, Z., Christensen, A., van Deurs, M., and Mosegaard, H.: Growth survival of larval and early juvenile Lesser Sandeel in patchy prey field in the North Sea: An examination using individual-based modeling, Ecol. Mod., 232, 78–90, 2012.

Gurkan, Z., Christensen, A., Maar, M., Müller, E. F., Madsen, K. S., Munk, P., and Mosegaard, H.: Spatio-Temporal Dynamics of Growth and Survival of Lesser Sandeel Early Life-Stages in the North Sea: Predictions from a Coupled Individual-Based and Hydrodynamic-Biogeochemical Model. Ecol. Mod., 250, 294–306, doi:10.1016/j.ecolmodel.2012.11.009, in press, 2013.

Hinrichsen, H.-H., Dickey-Collas, M., Huret, M., Peck, M. A., and Vikebo, F. B.: Evaluating the suitability of coupled biophysical models for fishery management, Ices J. Mar. Sci., 68, 1478–1487, doi:10.1093/icesjms/fsr056, 2011.

Holt, J., Butenschön, M., Wakelin, S. L., Artioli, Y., and Allen, J. I.: Oceanic controls on the primary production of the northwest European continental shelf: model experiments under recent past conditions and a potential future scenario, Biogeosciences, 9, 97–117, doi:10.5194/bg-9-97-2012, 2012.

Hufnagl, M. and Peck, M. A.: Physiological individual-based modelling of larval Atlantic herring (Clupea harengus) foraging and growth: insights on climate-driven life-history scheduling, ICES J. Mar. Sci., 68, 1170–1188, 2011

Huse, G. and Ottersen, G.: Forecasting recruitment and stock biomass of Northeast Arctic cod using neural networks, SAP Symposium on Fish Stock Assessments and Predictions, Bergen, Norway, 4–6 December 2000, Sci. Mar., 67, 325–335, 2003.

Jansen, T., Kristensen, K., Payne, M., Edwards, M., Schrum, C., and Pitois, S.: Long-Term Retrospective Analysis of Mackerel Spawning in the North Sea: A New Time Series and Modeling Approach to CPR Data, PLoS ONE, 7, e38758, doi:10.1371/journal.pone.0038758, 2012.

Jensen, H.: Settlement dynamics in the lesser sandeel Ammodytes marinus in the North Sea, PhD thesis, University of Aberdeen, 2001.

Jensen, H. and Rolev, A. M.: The Sandeel fishing grounds in the North Sea. Information about the foraging areas of the lesser sandeel Ammodytes marinus in the North Sea, Tech. rep., Danish Institute of Fisheries Research, working document prepared for the BECAUSE project, 2004.

Jensen, H., Rindorf, A., Wright, P. J., and Mosegaard, H.: Inferring the location and scale of mixing between habitat areas of lesser sandeel through information from the fishery, Ices J. Mar. Sci., 68, 43–51, doi:10.1093/icesjms/fsq154, 2011.

Kenny, A. J., Skjoldal, H. R., Engelhard, G. H., Kershaw, P. J., and Reid, J. B.: An integrated approach for assessing the relative significance of human pressures and environmental forcing on the status of Large Marine Ecosystems, ICES Annual Science Conference, Helsinki, Finland, 2007, Prog. Oceanogr., 81, 132–148, doi:10.1016/j.pocean.2009.04.007, 2009.

Kishi, M. J., Ito, S.-I., Megrey, B. A., Rose, K. A., and Werner, F. E.: A review of the NEMURO and NEMURO.FISH models and their application to marine ecosystem investigations, J. Oceanogr., 67, 3–16, doi:10.1007/s10872-011-0009-4, 2011.

Larsen, J., Hoyer, J. L., and She, J.: Validation of a hybrid optimal interpolation and Kalman filter scheme for sea surface temperature assimilation, J. Mar. Sci., 65, 122–133, 2007.

Lehodey, P., Senina, I., and Murtugudde, R.: A Spatial Ecosystem And Populations Dynamics Model (SEAPODYM) – Modelling of tuna and tuna-like populations, Prog. Oceanogr., 78, 304–318, 2008.

Lehodey P., Murtugudde R., and Senina I.:. Bridging the gap from ocean models to population dynamics of large marine predators: a model of mid-trophic functional groups, Prog. Oceanogr., 84, 69–84, 2010.

Letcher, B. H., Rice, J. A., Crowder, L. B., and Rose, K. A.: Variability in survival of larval fish: Disentangling components with a generalized individual-based model, Can. J. Fish. Aquat. Sci., 53, 787–801, 1996.

Levin, S. and Lubchenco, J.: Resilience, robustness, and marine ecosystem-based management, Bioscience, 58, 27–32, 2008.

Lewy, P., Nielsen, A., and Gislason, H.: Stock dynamics of sandeel in the North Sea and sub-regions including uncertainties, Fish. Res., 68, 237–248, doi:10.1016/j.fishres.2003.12.004, 2004.

Maar, M., Møller, E. F., Gurkan, Z., Jonasdottir, S. H., and Nielsen, T. G.: Sensitivity of Calanus spp. copepods to environmental changes in the North Sea using life-stage structured models, Prog. Oceanogr., doi:10.1016/j.pocean.2012.10.004, in press, 2013.

Macer, C. T.: Sand eels (Ammodytidae) in the south-western North Sea; their biology and fishery, Fish. Invest. II, 24, 1–55, 1966.

Mariani, P., Dobrynin, M., Christensen, A., Munk, P., and MacKenzie, B. R.: Modelling fish larval transport and aggregation processes in the North Sea, in preparation, 2013.

Megrey, B., Lee, Y., and Macklin, S.: Comparative analysis of statistical tools to identify recruitment-environment relationships and forecast recruitment strength, ICES Symposium on Influence of Climate Change on North Atlantic Fish Stocks, Bergen, Norway, 11–14 May 2004, Ices J. Mar. Sci., 62, 1256–1269, doi:10.1016/j.icesjms.2005.05.018, 2005.

Moellmann, C., Diekmann, R., Muller-Karulis, B., Kornilovs, G., Plikshs, M., and Axe, P.: Reorganization of a large marine ecosystem due to atmospheric and anthropogenic pressure: a discontinuous regime shift in the Central Baltic Sea, Glob. Change Biol., 15, 1377–1393, doi:10.1111/j.1365-2486.2008.01814.x, 2009.

Murray, J. D.: Mathematical Biology: I. An Introduction, Springer Verlag, 2002.

MyOcean: MyOcean EU project (FP7-SPACE-2007-1), available at: http://www.myocean.eu.org/, 2009–2012.

Payne, M. R., Egan, A., Fassler, S. M. M., Hatun, H., Holst, J. C., Jacobsen, J. A., Slotte, A., and Loeng, H.: The rise and fall of the NE Atlantic blue whiting (Micromesistius poutassou), Mar. Biol. Res., 8, 475–487, 2012

Radach, G. and Moll, A.: Review of three-dimensional ecological modelling related to the North Sea shelf system, Part 2, Oceanogr. Mar. Biol., 44, 1–60, 2006.

Robinson, A. R. and Lermusiaux, P. F. J: Overview of Data Assimilation, Harvard Reports in Physical/Interdisciplinary Ocean Science 62, Cambridge, Massachusetts, 2000.

Senina, I., Sibert, J., and Lehodey, P.: Parameter estimation for basin-scale ecosystem-linked population models of large pelagic predators: application to skipjack tuna, Prog. Oceanogr., 78, 319–335, 2008.

Siddorn, J. R., Allen, J. I., Blackford, J. C., Gilbert, F. J., Holt, J. T., Holt, M. W., Osborne, J. P., Proctor, R., and Mills, D. K.: Modelling the hydrodynamics and ecosystem of the North-West European continental shelf for operational oceanography, 36th International Liege Colloquium on Ocean Dynamics, Liege, Belgium, 3–7 May 2004, J. Marine Syst., 65, 417–429, doi:10.1016/j.jmarsys.2006.01.018, 2007.

Suryanarayana, I., Braibanti, A., Rao, R. S., Ramam, V. A., Sudarsan, D., and Rao, G. N.: Neural networks in fisheries research, Fish. Res., 92, 115–139, doi:10.1016/j.fishres.2008.01.012, 2008.

van Deurs, M., van Hal, R., Tomczak, M. T., Jonasdottir, S. H., and Dolmer, P.: Recruitment of lesser sandeel Ammodytes marinus in relation to density dependence and zooplankton composition, Mar. Ecol.-Prog. Ser., 381, 249–258, doi:10.3354/meps07960, 2009.

West, G. B., Brown, J. H., and Enquist, B. J.: A general model for ontogenetic growth, Nature, 413, 628–631, 2001.

WGNSSK: Report of the Working Group on the Assessment of Demersal Stocks in the North Sea and Skagerrak (WGNSSK), 4–10 May 2011, ICES Headquarters, Copenhagen., Tech. rep., ICES, ICES CM 2011/ACOM:13, 2011.

Wright, P. J. and Bailey, M. C.: Timing of hatching in Ammodytes marinus from Shetland waters and its significance to early growth and survivorship, Mar. Biol., 126, 143–152, 1996.